LATTICE DYNAMICS OF CHROMIUM (Cr) AND NIOBIUM (Nb): DFT AND IFCs APPROACH

[1]OKOCHA G.O., [2]OTOBO S.I. and [3]ALEBU O.

[1,3]**Department of Science Laboratory Technology, School of Applied Sciences and Technology, Auchi Polytechnic, Auchi**.
[2]**Department of Basic Science, School of General Studies, Auchi Polytechnic, Auchi**

Abstract

The phonon dispersion curves of Chromium (Cr) and Niobium (Nb) have been calculated from computational approach (first principle using density functional theory) with the exchange correlation functional and analytical (IFCs technique using Born – von Kármán model) with different numbers of interacting nearest-neighbours (NN). The different branches of the phonon band structure follow from the eigen values after diagonalizing the dynamical matrix. The phonon frequencies in the first Brillouin zone were calculated along the directions of high symmetry, $\Gamma \rightarrow H$, $H \rightarrow P$, $P \rightarrow \Gamma$ and $\Gamma \rightarrow N$. Obtain also are the thermodynamic properties from first principle (QUANTUM ESPRESSO) and analytical. It is observed that the phonon dispersion curve of Cr and Nb from IFCs calculation gave a fair agreement with experiment just like the first principle calculations.

1. INTRODUCTION

In solids, a vast number of physical properties hinge on the behaviour of their lattice-dynamics and it follows that the force model, if given a good fit to the dispersion curves in every principal symmetry direction foretell brilliantly all other properties of the lattice dynamics of the material [1]. The understanding of these properties in terms of phonons is thought-out to be amongst the persuading piece validating the correctness of the current quantum picture of solids [2].

The fundamental theory of the vibrations of lattice was established in the thirties. The textbook reference in this field, the work of Born and Huang [3] which lack the connections with the electronic properties but is rather involved with initiating the general properties of the matrices of the dynamics—like their analytical properties and/or symmetry. A study of the systematic connections of the electronic properties started from the seventies [4, 5]. The importance in the connection associated with the properties of the lattice dynamics of a system and the electrons can never be overemphasized because, in the exploitation of these connection makes it feasible in computing the properties of the lattice dynamics of specific systems. The dynamics of lattice allows one to express the contributions of the internal strains in relation to the microscopic quantities like optoacoustical couplings and effective ionic charges [6]. As well as the models of elastic-force, [7, 8] obtained from the method of orthogonalized plane-wave, the method of pseudopotential. This was in different forms improved upon by several authors [9, 10, 11, 12,13]. In the calculation of the properties of lattice dynamics, this has proved an effective means for a lot of simple metals. The idea of quantum defect by Heine-Abarenkov [12, 14] was used to study certain electronic properties and the dispersion curve of several transition metals by Animalu [15, 16], by formulating the transition metal model potential (TMMP). Animalu discovered that in FCC metals the results from the experiment agrees with theoretical results. This was different for BCC transition metals where the branch of transverse crosses over the

Correspondence Author: Okocha G.A., Email: obitex5555@gmail.com, Tel: +2348038587711
Transactions of the Nigerian Association of Mathematical Physics Volume 18, (January - December, 2022), 21-36

21

longitudinal before the zone boundary. The first principle prediction of the dispersion curves of phonon of noble and transition metals has been a tough problem which has not been totally resolved. DFPT [17] has often been used in resolving problems [18, 19, 20, 21, 22] but has succeeded to some extent in different metals. The prediction of the phonon curves of simple metals like aluminium is easy, and was amongst those studied first using first principle method [22]. Also, in reasonable agreement with experimental results are Iridium, nickel and gold with exchange and correlation functional not below one, while several metals have not achieved this feat. Copper a noble metal is a typical example, whose theoretical phonon curves are with huge errors when compared to experiment [23, 24, 25, 20, 21]. Lately the investigation on the interaction of electron-phonon and the pairing mechanism in the superconducting Ca-intercalated bilayer graphene (C_6CaC_6) using the first principle anisotropic Eliashberg theory with Coulomb interactions was carried out [26]. The inelastic helium atom scattering (HAS) and high-resolution electron energy loss spectroscopy (HREELS) was employed to study the phonon dispersion of graphene grown on some single crystal metal surfaces [27]. The thermal properties of molecular crystals were computed by the using first principle quantum-mechanical theoretical framework which merge dispersion-corrected density-functional-theory (DFT-D), quasi-harmonic approximation, harmonic phonon dispersion, to the lattice dynamics for thermodynamic functions and thermal expansion, and quasi-static approximation for anisotropic thermos-elasticity [28]. The challenge here is to determine and improve on existing techniques employed to determine the lattice dynamics of Cr and Nb using computational approach (first principle or ab-initio – QUANTUM ESPRESSO) and analytical approach (interatomic force constants – IFCs) and compare with experiment. Also calculated are their thermodynamic properties.

2.0   THEORETICAL FORMALISM
2.1   ANALYTICAL (IFCs) PROCEDURE
The Born-von Kármán theory was applied by assigning a force-constant matrix to each of the nearest neighbours of the atom considered, constructing the dynamical matrix from the individual force-constant matrices, and then solving the dynamical matrix for the phonon energies and the associated phonon polarizations.

INTERATOMIC FORCE CONSTANTS (IFCs)
The frequencies of the phonon of any material are typically somewhat a smooth function of the wave vector. Thus, for complete phonon dispersion an appropriate interpolation technique is needed. By Fourier analysis, the smoother the phonon dispersions considering the real space IFCs, the shorter the range of the real space:

$$\tilde{C}_{st}^{\alpha\beta}(\vec{R}) = \frac{1}{N_c}\sum e^{i\vec{q}\cdot\vec{R}}\tilde{C}_{st}^{\alpha\beta}(\vec{q}) \qquad (1)$$

Thus, real space IFCs, i.e. the force constants between atoms of a system in a real space is easy and achievable using a set of matrix force constants computed and presented in a table on an even grid of points within a reciprocal space. The *fast Fourier transform* (FFT) technique [29] is the most effective way of computing numerically all these Fourier transforms. After obtaining the force constants between atoms of a system in real-space, then the dynamical matrices in reciprocal space (and, hence, vibrational) frequencies can be obtained at any wave vector (not necessarily contained in the original grid) by FFT. The shorter the range of real space force constants, the coarser will be the reciprocal space grid needed for such Fourier interpolation.

CONSTRUCTION OF THE DYNAMICAL MATRIX
The phonon frequencies are given by the solution of the secular determinant

$$\left|D_{ij}(\vec{q}) - m\omega^2 I\right| = 0 \qquad (2)$$

Where m is the mass of the ion, ω is the phonon frequency, $D_{ij}(\vec{q})$ is the dynamical matrix elements and I is a 3×3 unit matrix. The elements of the dynamical matrix are a matrix as shown below

$$D_{ij} = \begin{pmatrix} D_{xx}(\vec{q}) & D_{xy}(\vec{q}) & D_{xz}(\vec{q}) \\ D_{yx}(\vec{q}) & D_{yy}(\vec{q}) & D_{yz}(\vec{q}) \\ D_{zx}(\vec{q}) & D_{zy}(\vec{q}) & D_{zz}(\vec{q}) \end{pmatrix} \qquad (3)$$

Once the force constant matrices have been determined the elements of the dynamical matrix are evaluated. This gives for the diagonal matrix elements of the first nearest to sixth nearest neighbours dynamical matrix as:

$$
D_{xx}(\vec{q}) = \frac{1}{M}\left\{
\begin{aligned}
&8\alpha_1 + 2\alpha_2 + 4\beta_2 + 8\alpha_3 + 4\beta_3 + 8\alpha_4 + 16\beta_4 + 8\alpha_5 + 2\alpha_6 + 4\beta_6 + 8\alpha_7 + 16\beta_7 \\
&+ 8\alpha_8 + 8\beta_8 + 8\gamma_8 + 8\alpha_9 + 16\beta_9 + 8\alpha_{10} - 8\alpha_1 \cos\left(\frac{aq_x}{2}\right)\cos\left(\frac{aq_y}{2}\right)\cos\left(\frac{aq_z}{2}\right) \\
&- 2\alpha_2 \cos(aq_x) - 2\beta_2 \cos(aq_y) - 2\beta_2 \cos(aq_z) - 4\alpha_3 \cos(aq_x)\cos(aq_y) \\
&- 4\alpha_3 \cos(aq_x)\cos(aq_z) - 4\beta_3 \cos(aq_x)\cos(aq_y) - 8\alpha_4 \cos\left(\frac{3aq_x}{2}\right)\cos\left(\frac{aq_y}{2}\right)\cos\left(\frac{aq_z}{2}\right) \\
&- 8\beta_4 \cos\left(\frac{aq_x}{2}\right)\cos\left(\frac{3aq_y}{2}\right)\cos\left(\frac{aq_z}{2}\right) - 8\beta_4 \cos\left(\frac{aq_x}{2}\right)\cos\left(\frac{aq_y}{2}\right)\cos\left(\frac{3aq_z}{2}\right) \\
&- 8\alpha_5 \cos(aq_x)\cos(aq_y)\cos(aq_z) - 2\alpha_6 \cos(2aq_x) - 2\beta_6 \cos(2aq_y) - 2\beta_6 \cos(2aq_z) \\
&- 8\alpha_7 \cos\left(\frac{aq_x}{2}\right)\cos\left(\frac{3aq_y}{2}\right)\cos\left(\frac{3aq_z}{2}\right) - 8\beta_7 \cos\left(\frac{3aq_x}{2}\right)\cos\left(\frac{3aq_y}{2}\right)\cos\left(\frac{aq_z}{2}\right) \\
&- 8\beta_7 \cos\left(\frac{3aq_x}{2}\right)\cos\left(\frac{3aq_y}{2}\right)\cos\left(\frac{aq_z}{2}\right) - 4\alpha_8 \cos(2aq_x)\cos(aq_y) - 4\alpha_8 \cos(2aq_x)\cos(aq_z) \\
&- 4\gamma_8 \cos(2aq_z)\cos(aq_y) - 4\gamma_8 \cos(2aq_y)\cos(aq_z) - 4\beta_8 \cos(aq_x)\cos(2aq_y) \\
&- 4\beta_8 \cos(aq_x)\cos(2aq_z) - 8\alpha_9 \cos(2aq_x)\cos(aq_y)\cos(aq_z) - 8\beta_9 \cos(aq_x)\cos(2aq_y)\cos(aq_z) \\
&- 8\beta_9 \cos(aq_x)\cos(aq_y)\cos(2aq_z) - 8\alpha_{10}\cos\left(\frac{3aq_x}{2}\right)\cos\left(\frac{3aq_y}{2}\right)\cos\left(\frac{3aq_z}{2}\right)
\end{aligned}
\right\}
$$

(4)

$$
D_{yy}(\vec{q}) = \frac{1}{M}\left\{
\begin{aligned}
&8\alpha_1 + 2\alpha_2 + 4\beta_2 + 8\alpha_3 + 4\beta_3 + 8\alpha_4 + 16\beta_4 + 8\alpha_5 + 2\alpha_6 + 4\beta_6 + 8\alpha_7 + 16\beta_7 \\
&+ 8\alpha_8 + 8\beta_8 + 8\gamma_8 + 8\alpha_9 + 16\beta_9 + 8\alpha_{10} - 8\alpha_1 \cos\left(\frac{aq_x}{2}\right)\cos\left(\frac{aq_y}{2}\right)\cos\left(\frac{aq_z}{2}\right) \\
&- 2\alpha_2 \cos(aq_y) - 2\beta_2 \cos(aq_x) - 2\beta_2 \cos(aq_z) - 4\alpha_3 \cos(aq_x)\cos(aq_y) \\
&- 4\alpha_3 \cos(aq_y)\cos(aq_z) - 4\beta_3 \cos(aq_x)\cos(aq_z) - 8\alpha_4 \cos\left(\frac{aq_x}{2}\right)\cos\left(\frac{3aq_y}{2}\right)\cos\left(\frac{aq_z}{2}\right) \\
&- 8\beta_4 \cos\left(\frac{3aq_x}{2}\right)\cos\left(\frac{aq_y}{2}\right)\cos\left(\frac{aq_z}{2}\right) - 8\beta_4 \cos\left(\frac{aq_x}{2}\right)\cos\left(\frac{aq_y}{2}\right)\cos\left(\frac{3aq_z}{2}\right) \\
&- 8\alpha_5 \cos(aq_x)\cos(aq_y)\cos(aq_z) - 2\alpha_6 \cos(2aq_y) - 2\beta_6 \cos(2aq_x) - 2\beta_6 \cos(2aq_z) \\
&- 8\alpha_7 \cos\left(\frac{3aq_x}{2}\right)\cos\left(\frac{aq_y}{2}\right)\cos\left(\frac{3aq_z}{2}\right) - 8\beta_7 \cos\left(\frac{aq_x}{2}\right)\cos\left(\frac{3aq_y}{2}\right)\cos\left(\frac{3aq_z}{2}\right) \\
&- 8\beta_7 \cos\left(\frac{3aq_x}{2}\right)\cos\left(\frac{3aq_y}{2}\right)\cos\left(\frac{aq_z}{2}\right) - 4\alpha_8 \cos(2aq_y)\cos(aq_z) - 4\alpha_8 \cos(aq_x)\cos(2aq_y) \\
&- 4\gamma_8 \cos(2aq_x)\cos(aq_z) - 4\gamma_8 \cos(2aq_x)\cos(aq_z) - 4\beta_8 \cos(2aq_x)\cos(aq_y) \\
&- 4\beta_8 \cos(aq_y)\cos(2aq_z) - 8\alpha_9 \cos(aq_x)\cos(2aq_y)\cos(aq_z) - 8\beta_9 \cos(2aq_x)\cos(aq_y)\cos(aq_z) \\
&- 8\beta_9 \cos(aq_x)\cos(aq_y)\cos(2aq_z) - 8\alpha_{10}\cos\left(\frac{3aq_x}{2}\right)\cos\left(\frac{3aq_y}{2}\right)\cos\left(\frac{3aq_z}{2}\right)
\end{aligned}
\right\}
$$

(5)

$$
D_{zz}(\vec{q}) = \frac{1}{M}\left\{
\begin{aligned}
&8\alpha_1 + 2\alpha_2 + 4\beta_2 + 8\alpha_3 + 4\beta_3 + 8\alpha_4 + 16\beta_4 + 8\alpha_5 + 2\alpha_6 + 4\beta_6 + 8\alpha_7 + 16\beta_7 \\
&+ 8\alpha_8 + 8\beta_8 + 8\gamma_8 + 8\alpha_9 + 16\beta_9 + 8\alpha_{10} - 8\alpha_1 \cos\left(\frac{aq_x}{2}\right)\cos\left(\frac{aq_y}{2}\right)\cos\left(\frac{aq_z}{2}\right) \\
&- 2\alpha_2 \cos(aq_z) - 2\beta_2 \cos(aq_x) - 2\beta_2 \cos(aq_y) - 4\alpha_3 \cos(aq_x)\cos(aq_z) \\
&- 4\alpha_3 \cos(aq_y)\cos(aq_z) - 4\beta_3 \cos(aq_x)\cos(aq_y) - 8\alpha_4 \cos\left(\frac{aq_x}{2}\right)\cos\left(\frac{aq_y}{2}\right)\cos\left(\frac{3aq_z}{2}\right) \\
&- 8\beta_4 \cos\left(\frac{3aq_x}{2}\right)\cos\left(\frac{aq_y}{2}\right)\cos\left(\frac{aq_z}{2}\right) - 8\beta_4 \cos\left(\frac{aq_x}{2}\right)\cos\left(\frac{3aq_y}{2}\right)\cos\left(\frac{aq_z}{2}\right) \\
&- 8\alpha_5 \cos(aq_x)\cos(aq_y)\cos(aq_z) - 2\alpha_6 \cos(2aq_z) - 2\beta_6 \cos(2aq_y) - 2\beta_6 \cos(2aq_x) \\
&- 8\alpha_7 \cos\left(\frac{3aq_x}{2}\right)\cos\left(\frac{3aq_y}{2}\right)\cos\left(\frac{aq_z}{2}\right) - 8\beta_7 \cos\left(\frac{aq_x}{2}\right)\cos\left(\frac{3aq_y}{2}\right)\cos\left(\frac{3aq_z}{2}\right) \\
&- 8\beta_7 \cos\left(\frac{3aq_x}{2}\right)\cos\left(\frac{aq_y}{2}\right)\cos\left(\frac{3aq_z}{2}\right) - 4\alpha_8 \cos(aq_x)\cos(2aq_z) - 4\alpha_8 \cos(aq_y)\cos(2aq_z) \\
&- 4\gamma_8 \cos(aq_x)\cos(2aq_y) - 4\gamma_8 \cos(2aq_x)\cos(aq_y) - 4\beta_8 \cos(2aq_x)\cos(aq_z) \\
&- 4\beta_8 \cos(2aq_y)\cos(aq_z) - 8\alpha_9 \cos(aq_x)\cos(aq_y)\cos(2aq_z) - 8\beta_9 \cos(2aq_x)\cos(aq_y)\cos(aq_z) \\
&- 8\beta_9 \cos(aq_x)\cos(2aq_y)\cos(aq_z) - 8\alpha_{10}\cos\left(\frac{3aq_x}{2}\right)\cos\left(\frac{3aq_y}{2}\right)\cos\left(\frac{3aq_z}{2}\right)
\end{aligned}
\right\}
$$

(6)

And the off - diagonal matrix elements of the first nearest to sixth nearest neighbour dynamical matrix as:

$$D_{xy} = \frac{1}{M} \left\{ \begin{array}{l} 8\beta_1 \sin\left(\frac{aq_x}{2}\right)\sin\left(\frac{aq_y}{2}\right)\cos\left(\frac{aq_z}{2}\right) + 4\gamma_3 \sin(aq_x)\sin(aq_y) \\[2mm] + 8\gamma_4 \sin\left(\frac{3aq_x}{2}\right)\sin\left(\frac{aq_y}{2}\right)\cos\left(\frac{aq_z}{2}\right) + 8\gamma_4 \sin\left(\frac{aq_x}{2}\right)\sin\left(\frac{3aq_y}{2}\right)\cos\left(\frac{aq_z}{2}\right) \\[2mm] + 8\delta_4 \sin\left(\frac{aq_x}{2}\right)\sin\left(\frac{aq_y}{2}\right)\cos\left(\frac{3aq_z}{2}\right) + 8\beta_5 \sin(aq_x)\sin(aq_y)\cos(aq_z) \\[2mm] + 8\gamma_7 \sin\left(\frac{aq_x}{2}\right)\sin\left(\frac{3aq_y}{2}\right)\cos\left(\frac{3aq_z}{2}\right) + 8\gamma_7 \sin\left(\frac{3aq_x}{2}\right)\sin\left(\frac{aq_y}{2}\right)\cos\left(\frac{3aq_z}{2}\right) \\[2mm] + 8\delta_7 \sin\left(\frac{3aq_x}{2}\right)\sin\left(\frac{3aq_y}{2}\right)\cos\left(\frac{aq_z}{2}\right) + 4\delta_8 \sin(2aq_x)\sin(aq_y) \\[2mm] + 4\delta_8 \sin(aq_x)\sin(2aq_y) + 8\gamma_9 \sin(2aq_x)\sin(aq_y)\cos(aq_z) \\[2mm] + 8\gamma_9 \sin(aq_x)\sin(2aq_y)\cos(aq_z) + 8\delta_9 \sin(aq_x)\sin(aq_y)\cos(2aq_z) \\[2mm] + 8\beta_{10} \sin\left(\frac{3aq_x}{2}\right)\sin\left(\frac{3aq_y}{2}\right)\cos\left(\frac{3aq_z}{2}\right) \end{array} \right\}$$

(7)

$$D_{xz} = \frac{1}{M} \left\{ \begin{array}{l} 8\beta_1 \sin\left(\frac{aq_x}{2}\right)\sin\left(\frac{aq_z}{2}\right)\cos\left(\frac{aq_y}{2}\right) + 4\gamma_3 \sin(aq_x)\sin(aq_z) \\[2mm] + 8\gamma_4 \sin\left(\frac{3aq_x}{2}\right)\sin\left(\frac{aq_z}{2}\right)\cos\left(\frac{aq_y}{2}\right) + 8\gamma_4 \sin\left(\frac{aq_x}{2}\right)\sin\left(\frac{3aq_z}{2}\right)\cos\left(\frac{aq_y}{2}\right) \\[2mm] + 8\delta_4 \sin\left(\frac{aq_x}{2}\right)\sin\left(\frac{aq_z}{2}\right)\cos\left(\frac{3aq_y}{2}\right) + 8\beta_5 \sin(aq_x)\sin(aq_z)\cos(aq_y) \\[2mm] + 8\gamma_7 \sin\left(\frac{aq_x}{2}\right)\sin\left(\frac{3aq_z}{2}\right)\cos\left(\frac{3aq_y}{2}\right) + 8\gamma_7 \sin\left(\frac{3aq_x}{2}\right)\sin\left(\frac{aq_z}{2}\right)\cos\left(\frac{3aq_y}{2}\right) \\[2mm] + 8\delta_7 \sin\left(\frac{3aq_x}{2}\right)\sin\left(\frac{3aq_z}{2}\right)\cos\left(\frac{aq_y}{2}\right) + 4\delta_8 \sin(2aq_x)\sin(aq_z) \\[2mm] + 4\delta_8 \sin(aq_x)\sin(2aq_z) + 8\gamma_9 \sin(2aq_x)\sin(aq_z)\cos(aq_y) \\[2mm] + 8\gamma_9 \sin(aq_x)\sin(2aq_z)\cos(aq_y) + 8\delta_9 \sin(aq_x)\sin(aq_z)\cos(2aq_y) \\[2mm] + 8\beta_{10} \sin\left(\frac{3aq_x}{2}\right)\sin\left(\frac{3aq_z}{2}\right)\cos\left(\frac{3aq_y}{2}\right) \end{array} \right\}$$

(8)

$$D_{yz} = \frac{1}{M} \left\{ \begin{array}{l} 8\beta_1 \sin\left(\frac{aq_y}{2}\right)\sin\left(\frac{aq_z}{2}\right)\cos\left(\frac{aq_x}{2}\right) + 4\gamma_3 \sin(aq_y)\sin(aq_z) \\[2mm] + 8\gamma_4 \sin\left(\frac{3aq_y}{2}\right)\sin\left(\frac{aq_z}{2}\right)\cos\left(\frac{aq_x}{2}\right) + 8\gamma_4 \sin\left(\frac{aq_y}{2}\right)\sin\left(\frac{3aq_z}{2}\right)\cos\left(\frac{aq_x}{2}\right) \\[2mm] + 8\delta_4 \sin\left(\frac{aq_z}{2}\right)\sin\left(\frac{aq_y}{2}\right)\cos\left(\frac{3aq_x}{2}\right) + 8\beta_5 \sin(aq_y)\sin(aq_z)\cos(aq_z) \\[2mm] + 8\gamma_7 \sin\left(\frac{aq_y}{2}\right)\sin\left(\frac{3aq_z}{2}\right)\cos\left(\frac{3aq_x}{2}\right) + 8\gamma_7 \sin\left(\frac{3aq_y}{2}\right)\sin\left(\frac{aq_z}{2}\right)\cos\left(\frac{3aq_x}{2}\right) \\[2mm] + 8\delta_7 \sin\left(\frac{3aq_y}{2}\right)\sin\left(\frac{3aq_z}{2}\right)\cos\left(\frac{aq_x}{2}\right) + 4\delta_8 \sin(2aq_y)\sin(aq_z) \\[2mm] + 4\delta_8 \sin(aq_y)\sin(2aq_z) + 8\gamma_9 \sin(2aq_y)\sin(aq_z)\cos(aq_x) \\[2mm] + 8\gamma_9 \sin(aq_y)\sin(2aq_z)\cos(aq_x) + 8\delta_9 \sin(aq_y)\sin(aq_z)\cos(2aq_x) \\[2mm] + 8\beta_{10} \sin\left(\frac{3aq_y}{2}\right)\sin\left(\frac{3aq_z}{2}\right)\cos\left(\frac{3aq_x}{2}\right) \end{array} \right\}$$

(9)

Where M denotes the mass of the element, and $D_{xy} = D_{yx}$, $D_{xz} = D_{zx}$ and $D_{yz} = D_{zy}$. The elements $\alpha_1, \beta_1, \ldots$ are the nearest neighbour parameters in a least-squares fit to the data. The force constants were also of great value as a simple mathematical description of the phonon spectrum [30] used this property in their method of calculating the phonon distribution function.

2.2 COMPUTATIONAL PROCEDURE

In the density functional theory (DFT)employed for Cr, the electron was treated using scalar relativistic ultra-soft *ab - initio* pseudopotential, within the applied self-consistent method. The computations are employed within the DFT using QUANTUM ESPRESSO code (opEn Source Package for Research in Electronic Structure, Simulation, and Optimization) [31, 32] for the exchange and correlation energy. The pseudo-wave functions expansion is carried out in plane waves with Kinetic Energy Cut-off Potential (ecutwfc) starting from (10 to 70) Ry at an interval of 5Ry. The converged value of the ecutwfc was found to be 60Ry for the three functionals used. Also, the K-points values are integrated over the BZ in the reciprocal space with uniform K-point meshes of $8 \times 8 \times 8$ points for both GGA (PBE) and GGA (PAW) and $9 \times 9 \times 9$ points for PW91. The self-consistency calculation was assumed to have converged when the difference in energy between subsequent iteration was 1.0×10^{-3} Ry.

2.3   CALCULATION OF THE THERMODYNAMIC PROPERTIES OF BCC METALS

Thermodynamic functions of solids are determined by their vibrational degrees of freedom of their lattice [33]. Thus, for the calculation of these thermodynamic functions requires a complete knowledge of the vibrational spectrum, with adequate accuracy [34]. The phonon contributions to the thermodynamic properties which include Helmholtz free energy ΔF, the internal energy ΔE, the constant-volume specific heat C_v, and the entropy S are computed for these bcc metals studied in this work within the temperature range of $0 - 800K$ with the following expressions:

For the Helmholtz free energy

$$\Delta F = 3nNK_BT\ln\left\{ \begin{array}{l} 2\sinh\left(\dfrac{\hbar\omega_1}{2K_BT}\right)g(\omega_1)\Delta\omega_1 + 2\sinh\left(\dfrac{\hbar\omega_2}{2K_BT}\right)g(\omega_2)\Delta\omega_2 \\ +\ldots+ 2\sinh\left(\dfrac{\hbar\omega_n}{2K_BT}\right)g(\omega_n)\Delta\omega_n \end{array} \right\} \tag{10}$$

For the internal energy we have

$$\Delta E = 3nN\dfrac{\hbar}{2}\ln\left\{ \begin{array}{l} \omega\coth\left(\dfrac{\hbar\omega}{2K_BT}\right)g(\omega_1)\Delta\omega_1 + \omega\coth\left(\dfrac{\hbar\omega}{2K_BT}\right)g(\omega_2)\Delta\omega_2 \\ +\ldots+ \omega\coth\left(\dfrac{\hbar\omega}{2K_BT}\right)g(\omega_n)\Delta\omega_n \end{array} \right\} \tag{11}$$

For the constant-volume specific heat we have

$$C_\upsilon = 3nNk_B\left\{ \begin{array}{l} \left(\dfrac{\hbar\omega_1}{2K_BT}\right)^2 \csc h^2\left(\dfrac{\hbar\omega_1}{2K_BT}\right)g(\omega_1)\Delta\omega_1 \\ +\left(\dfrac{\hbar\omega_2}{2K_BT}\right)^2 \csc h^2\left(\dfrac{\hbar\omega_2}{2K_BT}\right)g(\omega_2)\Delta\omega_2 +\ldots \\ +\left(\dfrac{\hbar\omega_n}{2K_BT}\right)^2 \csc h^2\left(\dfrac{\hbar\omega_n}{2K_BT}\right)g(\omega_n)\Delta\omega_n \end{array} \right\} \tag{12}$$

Finally, for the entropy we have

$$S = 3nNk_B\left\{ \begin{array}{l} \left[\dfrac{\hbar\omega_1}{2K_BT}\coth\dfrac{\hbar\omega_1}{2K_BT} - \ln\left(2\sinh\dfrac{\hbar\omega_1}{2K_BT}\right)\right]g(\omega)d\omega_1 \\ +\left[\dfrac{\hbar\omega_2}{2K_BT}\coth\dfrac{\hbar\omega_2}{2K_BT} - \ln\left(2\sinh\dfrac{\hbar\omega_2}{2K_BT}\right)\right]g(\omega)d\omega_2 \\ +\ldots+\left[\dfrac{\hbar\omega_n}{2K_BT}\coth\dfrac{\hbar\omega_n}{2K_BT} - \ln\left(2\sinh\dfrac{\hbar\omega_n}{2K_BT}\right)\right]g(\omega)d\omega_n \end{array} \right\} \tag{13}$$

Note: $\coth = \dfrac{1}{\tanh}$, $\csc h = \dfrac{1}{\sinh}$

Where K_B is the Boltzmann's constant, $\hbar$ is reduced Planck's constant

3.0   RESULTS AND DISCUSSION
3.1   DISCUSSION OF RESULTS

Figure 1, shows the phonon dispersion curve of Chromium (Cr) from IFCs calculated by with sixth nearest neighbours force constant fit to Born – von Kármán model matched with data from experiment. The data from experiment is presented in blue, green and red circles, with the red solid line calculations from IFCs. In Figure 2, the experimental data is shown as blue, green and red circles, the black solid curve shows the dispersion calculated using the GGA (PBE), the red solid curve shows the dispersion calculated using PW91 functional and the blue solid curve the dispersion calculated using the GGA (PAW). IFCs calculations of the phonon dispersions of Chromium showed that the 1-6th nearest neighbours dispersions calculated with (MAE 0.0367THz), percentage error (MARE 0.46%), whereas, the density functional theory (DFT) using GGA (PBE), PW91 and GGA (PAW) gave a larger MAE, percentage error (MARE) as (MAE 0.3475THz, MARE 4.39%), (MAE 2.0904THz, MARE 26.41%) and (MAE 0.1038THz, MARE 1.31%) respectively. Figure 3, shows the phonon dispersion curve of Niobium (Nb) from IFCs calculated by with tenth nearest neighbours force constant fit to Born – von Kármán model matched with data from experiment. The data from experiment is presented in blue, green and red circles, with the red solid line calculations from IFCs. In Figure 4, the experimental data is shown as blue, green and red circles, the black solid curve shows the dispersion calculated using the GGA (PBE), the red solid curve shows the dispersion calculated using LDA functional and the blue solid curve the dispersion calculated using the PW91. IFCs calculations of the phonon dispersions of Niobium (Nb) showed that the 1-10th nearest neighbours dispersions calculated with (MAE 0.2713THz), percentage error (MARE 5.07%), whereas, the density functional theory (DFT) using GGA (PBE), PW91 and LDA gave a larger MAE, percentage error (MARE) as (MAE 1.0427THz, MARE 19.50%), (MAE 0.5047THz, MARE 9.44%) and (MAE 2.0103THz, MARE 37.59%) respectively as shown in Tables2a and 2b. The interatomic force constant (IFCs) fit to Born – von Kármán model gave better results than the first principle (QUANTUM ESPRESSO) calculations. In the first principle calculations using DFT, the PW91 functional gave a better result compared to GGA (PBE) with the LDA worst of the functional. Also, the GGA (PBE) gave a better error to the lattice constant of 0.37% slightly above experiment while PW91 and LDA overestimated and underestimated by 0.85% and 1.56% respectively. Details of the extension of the force constants will be discussed in details somewhere else.

3.2   Thermodynamic properties

Figs. 5 and 9, shows an increase in the internal energy as temperature increases and also at 0K it is above zero. Figs. 6 and 10, shows a decrease in the free energy with increase in temperature whereas in Figs. 7 and 11, shows an increase in the entropy with an increase in temperature. In Figs. 8 and 12, the heat capacity on the other hand shows a rapid increase with temperature and approaches the Dulong-Petit limit at high temperature and at low temperature the graph obeys the T^3 and at very low temperature the graph obeys the linear law as can be found in literature.
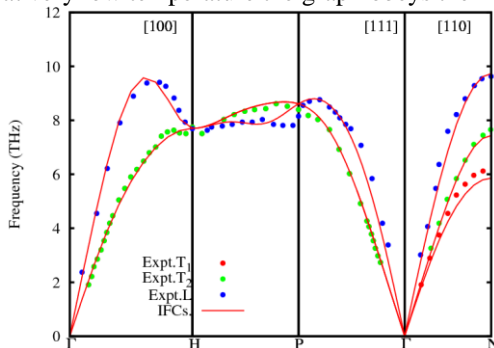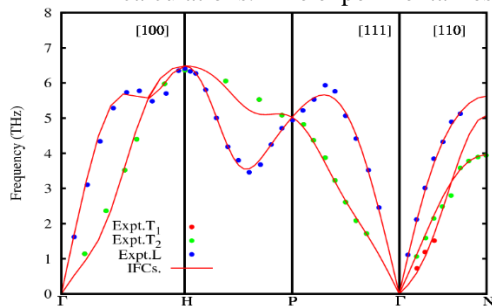

Fig 1: Chromium dispersion curves. The Red curves correspond to sixth nearest neighbours fit (IFCs). The experimental results [34] are shown by the symbols   and
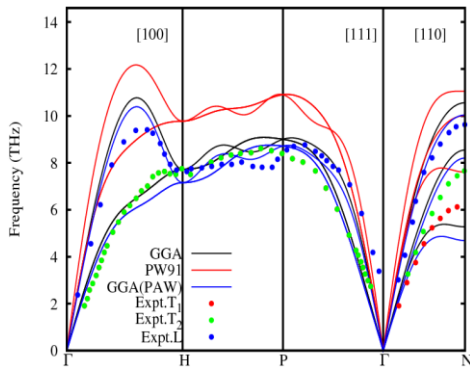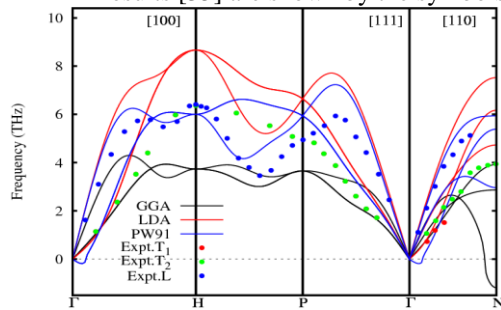
Fig 2: Chromium dispersion curves. GGA(PBE), PW91 and GGA(PAW) results from QUANTUM ESPRESSO calculations. The experimental results [34] are shown by the symbols   ,   and


Fig 3: Niobium dispersion curves. The Red curves correspond to tenth nearest neighbours fit (IFCs). The experimental results [35] are shown by the symbols   ,   and


Fig 4: Niobium dispersion curves. GGA (PBE), LDA and PW91 results from QUANTUM ESPRESSO calculations. The experimental results [36] are shown by the symbols   ,   and
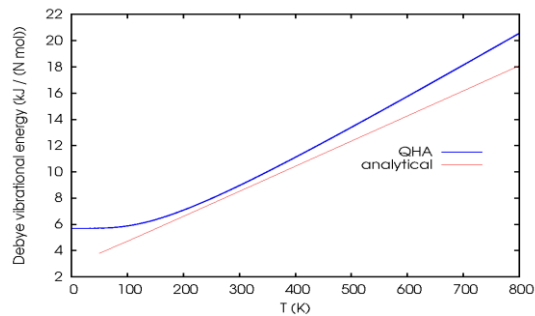
Fig 5: The internal energies ΔE of Chromium. Analytical (IFCs) calculated values in the pink line; First principle (QUANTUM ESPRESSO) calculated values in blue line
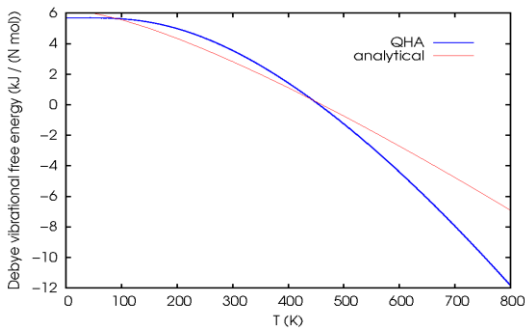
Fig 6: The Helmholtz free energies ΔF of Chromium. Analytical (IFCs) calculated values in the pink line; First principle (QUANTUM ESPRESSO) calculated values in blue line
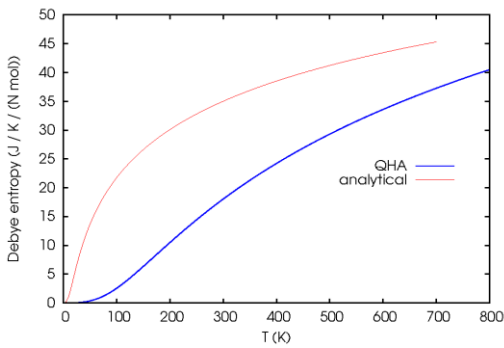
Fig 7: The entropy of Chromium. Analytical (IFCs) calculated values in the pink line; First principle (QUANTUM ESPRESSO) calculated values in blue line

Fig 8: The C_v for Chromium. Analytical (IFCs) in the pink line dispersion; First principle (QUANTUM ESPRESSO) calculated values in blue line
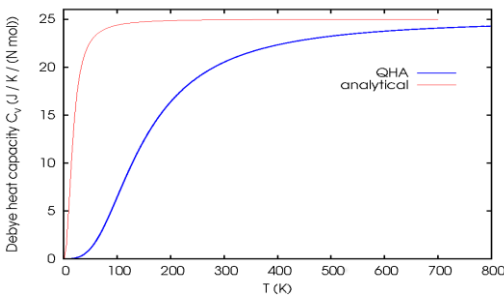

Fig 9: The internal energies ΔE of Niobium. Analytical (IFCs) calculated values in the pink line; First principle (QUANTUM ESPRESSO) calculated values in blue line

Fig 10: The Helmholtz free energies ΔF of Niobium. Analytical (IFCs) calculated values in the pink line; First principle (QUANTUM ESPRESSO) calculated values in blue line

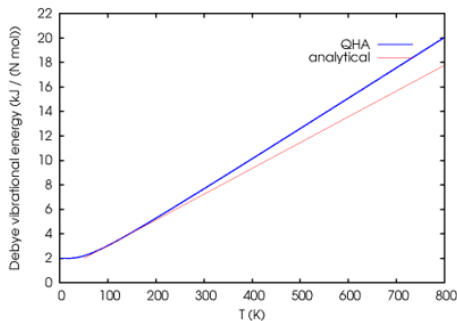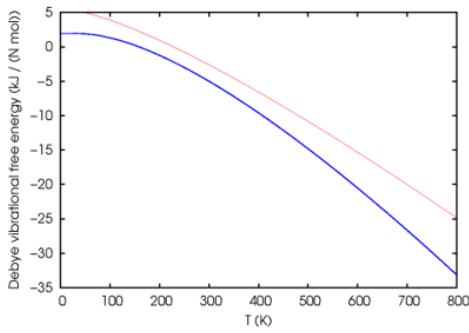

Fig 11: The entropy of Niobium. Analytical (IFCs) calculated values in the pink line; First principle (QUANTUM ESPRESSO) calculated values in blue line
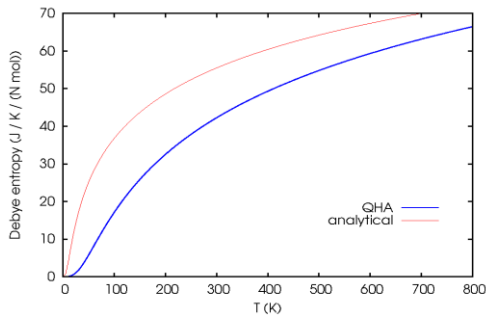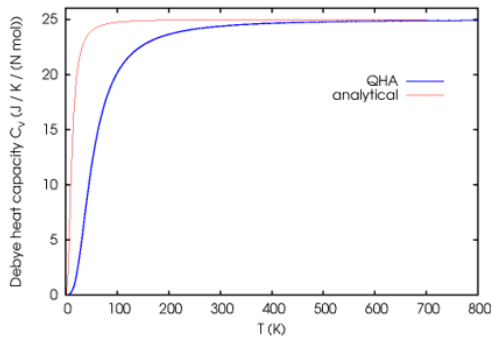

Fig 12: The C_v for Niobium. Analytical (IFCs) in the pink line dispersion; First principle (QUANTUM ESPRESSO) calculated values in blue line

Table 1: (a) Frequencies and calculated percentage errors at some high symmetry points for Chromium (Cs). (b) Calculated MAE and MARE for Chromium.

(a)

	a_T			FREQUENCY(THz)				
	$(a.u)$	H_L	H_T	P_L	P_T	N_L	N_{T_1}	N_{T_2}
GGA(PBE)	5.38	7.7202	7.7202	9.0062	9.0062	10.5606	5.2732	8.5501
PW91	5.38	9.7764	9.7764	10.9045	10.9045	11.0575	7.6052	10.0127
GGA(PAW)	5.42	7.1547	7.1547	8.7172	8.7172	10.0388	4.6895	8.2052
IFCs	-	7.7027	7.7027	8.6125	8.6125	9.7341	5.8594	7.4370
Expt. [a]	5.499	7.6919	7.7529	8.1541	8.3983	9.6279	6.1221	7.6570
				% Error				
GGA(PBE)	-2.16	0.37	0.42	10.45	7.24	9.69	13.87	11.66
PW91	-2.16	27.10	26.10	33.73	29.84	14.85	24.23	30.77
GGA(PAW)	-1.44	6.98	7.72	6.91	3.80	4.27	23.40	7.16
IFCs	-	0.14	0.65	5.73	2.55	1.10	4.29	2.87

(b)

	TOTAL	AVERAGE	$\pm(work - expt.)$(THz)	MAE (THz)	MARE (%)
GGA(PBE)	57.8367	8.2624	2.4325	0.3475	4.39
PW91	70.0372	10.0053	14.6330	2.0904	26.41
GGA(PAW)	54.6773	7.8110	0.7269	0.1038	1.31
IFCs	55.6609	7.9516	0.2567	0.0367	0.46
Expt. [a]	55.4042	7.9149	-	-	-

[a][33] (Experiment)

Table 2: (a) Frequencies and calculated percentage errors at some high symmetry points for Niobium (Nb), (b) Calculated MAE and MARE for Niobium.

(a)

	a_T (a.u)	H_L	FREQUENY (THz) H_T	P_L	P_T	N_L	N_{T_1}	N_{T_2}
GGA(PBE)	6.26	3.7351	3.7351	3.6545	3.6545	3.9142	-1.1877	2.8657
PW91	6.29	6.0028	6.0028	5.9395	5.9395	5.9346	2.9607	5.3798
LDA	6.14	8.6642	8.6642	6.6461	6.6461	7.5247	4.7297	6.1721
IFCs	-	6.4847	6.4847	5.0251	5.0251	5.6258	3.9595	5.0774
Expt. [b]	6.237	6.4105	6.3623	4.9436	5.0837	-	-	3.9409
			% Error					
GGA(PBE)	0.37	41.29	41.29	28.11	28.11	-	-	27.28
PW91	0.85	5.65	5.65	14.66	14.66	-	-	36.76
LDA	-1.56	36.18	36.18	30.73	30.73	-	-	56.62
IFCs	-	1.92	1.92	1.15	1.15	-	-	28.83

(b)

	TOTAL	AVERAGE	$\pm(wok - expt.)$(THz)	MAE (THz)	MARE (%)
GGA(PBE)	21.5274	3.5290	5.2136	1.0427	19.50
PW91	29.2644	5.8529	2.5234	0.5047	9.44
LDA	36.7927	7.3585	10.0517	2.0103	37.59
IFCs	28.0970	5.6194	1.3560	0.2712	5.07
Expt. [b]	26.7410	5.3482	-	-	-

[b][34] (Experiment)

Table 3: First - Sixth and First - Tenth nearest neighbours general force models for Chromium and Niobium respectively.

Position of neighbour	Force constant (dyn/cm)	Sixth nearest neighbours fit	Tenth nearest neighbours fit	Nearest neighbours
$\frac{a}{2}(1,1,1)$	α_1	14350	14140	First
$\frac{a}{2}(1,1,1)$	β_1	6930	8840	First
$\frac{a}{2}(2,0,0)$	α_2	37700	14160	Second
$\frac{a}{2}(2,0,0)$	β_2	-770	-3640	Second
$\frac{a}{2}(2,2,0)$	α_3	1380	2270	Third
$\frac{a}{2}(2,2,0)$	β_3	-500	-6380	Third
$\frac{a}{2}(2,2,0)$	γ_3	1490	760	Third
$\frac{a}{2}(3,1,1)$	α_4	-1910	3610	Fourth
$\frac{a}{2}(3,1,1)$	β_4	110	-750	Fourth
$\frac{a}{2}(3,1,1)$	γ_4	-370	1260	Fourth
$\frac{a}{2}(3,1,1)$	δ_4	750	-950	Fourth

Atomic Pair	Symbol	Okocha, Otobo and Alebu	Trans. Of NAMP	Neighbour
$\frac{a}{2}(2,2,2)$	α_5	**450**	**-1160**	**Fifth**
$\frac{a}{2}(2,2,2)$	β_5	530	-1330	Fifth
$\frac{a}{2}(4,0,0)$	α_6	-4	-7080	Sixth
$\frac{a}{2}(4,0,0)$	β_6	5	1320	Sixth
$\frac{a}{2}(1,3,3)$	α_7		-30	Seventh
$\frac{a}{2}(1,3,3)$	β_7		-100	Seventh
$\frac{a}{2}(1,3,3)$	γ_7		-170	Seventh
$\frac{a}{2}(1,3,3)$	δ_7		370	Seventh
$\frac{a}{2}(4,2,0)$	α_8		510	Eighth
$\frac{a}{2}(4,2,0)$	β_8		-270	Eighth
$\frac{a}{2}(4,2,0)$	γ_8		870	Eighth
$\frac{a}{2}(4,2,0)$	δ_8		-60	Eighth
$\frac{a}{2}(4,2,2)$	α_9		80	Ninth
$\frac{a}{2}(4,2,2)$	β_9		-40	Ninth
$\frac{a}{2}(4,2,2)$	γ_9		-2	Ninth
$\frac{a}{2}(4,2,2)$	δ_9		1	Ninth
$\frac{a}{2}(3,3,3)$	α_{10}		0	Tenth
$\frac{a}{2}(3,3,3)$	β_{10}		5	Tenth

Table 4: Force-constant matrices $\emptyset(0,l)$ corresponding to the first nearest to tenth nearest neighbours of the atom at the origin

Atomic Pair	$\phi(0,l)$	Atomic Pair	$\phi(0,l)$	Atomic Pair	$\phi(0,l)$
$0-1\ \frac{a}{2}(1,1,1)$ $\frac{a}{2}(-1,-1,-1)$	$-\begin{pmatrix} \alpha_1 & \beta_1 & \beta_1 \\ \beta_1 & \alpha_1 & \beta_1 \\ \beta_1 & \beta_1 & \alpha_1 \end{pmatrix}$	$0-2\ \frac{a}{2}(-1,1,1)$ $\frac{a}{2}(1,-1,-1)$	$-\begin{pmatrix} \alpha_1 & -\beta_1 & \beta_1 \\ -\beta_1 & \alpha_1 & -\beta_1 \\ \beta_1 & -\beta_1 & \alpha_1 \end{pmatrix}$	$0-3\ \frac{a}{2}(1,-1,1)$ $\frac{a}{2}(-1,1,-1)$	$-\begin{pmatrix} \alpha_1 & -\beta_1 & \beta_1 \\ -\beta_1 & \alpha_1 & -\beta_1 \\ \beta_1 & -\beta_1 & \alpha_1 \end{pmatrix}$
$0-4\ \frac{a}{2}(-1,-1,1)$ $\frac{a}{2}(1,1,-1)$	$-\begin{pmatrix} \alpha_1 & \beta_1 & -\beta_1 \\ \beta_1 & \alpha_1 & -\beta_1 \\ -\beta_1 & -\beta_1 & \alpha_1 \end{pmatrix}$	$0-5\ \frac{a}{2}(2,0,0)$ $\frac{a}{2}(-2,0,0)$	$-\begin{pmatrix} \alpha_2 & 0 & 0 \\ 0 & \beta_2 & 0 \\ 0 & 0 & \beta_2 \end{pmatrix}$	$0-6\ \frac{a}{2}(0,2,0)$ $\frac{a}{2}(0,-2,0)$	$-\begin{pmatrix} \beta_2 & 0 & 0 \\ 0 & \alpha_2 & 0 \\ 0 & 0 & \beta_2 \end{pmatrix}$
$0-7\ \frac{a}{2}(0,0,2)$ $\frac{a}{2}(0,0,-2)$	$-\begin{pmatrix} \beta_2 & 0 & 0 \\ 0 & \beta_2 & 0 \\ 0 & 0 & \alpha_2 \end{pmatrix}$	$0-8\ \frac{a}{2}(2,2,0)$ $\frac{a}{2}(-2,-2,0)$	$-\begin{pmatrix} \alpha_3 & \gamma_3 & 0 \\ \gamma_3 & \alpha_3 & 0 \\ 0 & 0 & \beta_3 \end{pmatrix}$	$0-9\ \frac{a}{2}(-2,2,0)$ $\frac{a}{2}(2,-2,0)$	$-\begin{pmatrix} \alpha_3 & -\gamma_3 & 0 \\ -\gamma_3 & \alpha_3 & 0 \\ 0 & 0 & \beta_3 \end{pmatrix}$

0 – 10 $\frac{a}{2}(0,2,2)$ $\frac{a}{2}(0,-2,-2)$	$-\begin{pmatrix}\beta_3 & 0 & 0\\0 & \alpha_3 & \gamma_3\\0 & \gamma_3 & \alpha_3\end{pmatrix}$	0 – 11 $\frac{a}{2}(0,-2,2)$ $\frac{a}{2}(0,2,-2)$	$-\begin{pmatrix}\beta_3 & 0 & 0\\0 & \alpha_3 & -\gamma_3\\0 & -\gamma_3 & \alpha_3\end{pmatrix}$	0 – 12 $\frac{a}{2}(2,0,2)$ $\frac{a}{2}(-2,0,-2)$	$-\begin{pmatrix}\alpha_3 & 0 & \gamma_3\\0 & \beta_3 & 0\\\gamma_3 & 0 & \alpha_3\end{pmatrix}$
0 – 13 $\frac{a}{2}(-2,0,2)$ $\frac{a}{2}(2,0,-2)$	$-\begin{pmatrix}\alpha_3 & 0 & -\gamma_3\\0 & \beta_3 & 0\\-\gamma_3 & 0 & \alpha_3\end{pmatrix}$	0 – 14 $\frac{a}{2}(3,1,1)$ $\frac{a}{2}(-3,-1,-1)$	$-\begin{pmatrix}\alpha_4 & \gamma_4 & \gamma_4\\\gamma_4 & \beta_4 & \delta_4\\\gamma_4 & \delta_4 & \beta_4\end{pmatrix}$	0 – 15 $\frac{a}{2}(-3,1,1)$ $\frac{a}{2}(3,-1,-1)$	$-\begin{pmatrix}\alpha_4 & -\gamma_4 & -\gamma_4\\-\gamma_4 & \beta_4 & \delta_4\\-\gamma_4 & \delta_4 & \beta_4\end{pmatrix}$
0 – 16 $\frac{a}{2}(3,1,-1)$ $\frac{a}{2}(-3,-1,1)$	$-\begin{pmatrix}\alpha_4 & \gamma_4 & -\gamma_4\\\gamma_4 & \beta_4 & -\delta_4\\-\gamma_4 & -\delta_4 & \beta_4\end{pmatrix}$	0 – 17 $\frac{a}{2}(3,-1,1)$ $\frac{a}{2}(-3,1,-1)$	$-\begin{pmatrix}\alpha_4 & -\gamma_4 & \gamma_4\\-\gamma_4 & \beta_4 & -\delta_4\\\gamma_4 & -\delta_4 & \beta_4\end{pmatrix}$	0 – 18 $\frac{a}{2}(1,3,1)$ $\frac{a}{2}(-1,-3,-1)$	$-\begin{pmatrix}\beta_4 & \gamma_4 & \delta_4\\\gamma_4 & \alpha_4 & \gamma_4\\\delta_4 & \gamma_4 & \beta_4\end{pmatrix}$
0 – 19 $\frac{a}{2}(1,-3,-1)$ $\frac{a}{2}(-1,3,1)$	$-\begin{pmatrix}\beta_4 & -\gamma_4 & -\delta_4\\-\gamma_4 & \alpha_4 & \gamma_4\\-\delta_4 & \gamma_4 & \beta_4\end{pmatrix}$	0 – 20 $\frac{a}{2}(1,3,-1)$ $\frac{a}{2}(-1,-3,1)$	$-\begin{pmatrix}\beta_4 & \gamma_4 & -\delta_4\\\gamma_4 & \alpha_4 & -\gamma_4\\-\delta_4 & -\gamma_4 & \beta_4\end{pmatrix}$	0 – 21 $\frac{a}{2}(1,-3,1)$ $\frac{a}{2}(-1,3,-1)$	$-\begin{pmatrix}\beta_4 & -\gamma_4 & \delta_4\\-\gamma_4 & \alpha_4 & -\gamma_4\\\delta_4 & -\gamma_4 & \beta_4\end{pmatrix}$
0 – 22 $\frac{a}{2}(1,1,3)$ $\frac{a}{2}(-1,-1,-3)$	$-\begin{pmatrix}\beta_4 & \delta_4 & \gamma_4\\\delta_4 & \beta_4 & \gamma_4\\\gamma_4 & \gamma_4 & \alpha_4\end{pmatrix}$	0 – 23 $\frac{a}{2}(1,1,-3)$ $\frac{a}{2}(-1,-1,3)$	$-\begin{pmatrix}\beta_4 & \delta_4 & -\gamma_4\\\delta_4 & \beta_4 & -\gamma_4\\-\gamma_4 & -\gamma_4 & \alpha_4\end{pmatrix}$	0 – 24 $\frac{a}{2}(-1,1,3)$ $\frac{a}{2}(1,-1,-3)$	$-\begin{pmatrix}\beta_4 & -\delta_4 & -\gamma_4\\-\delta_4 & \beta_4 & \gamma_4\\-\gamma_4 & \gamma_4 & \alpha_4\end{pmatrix}$
0 – 25 $\frac{a}{2}(1,-1,3)$ $\frac{a}{2}(-1,1,-3)$	$-\begin{pmatrix}\beta_4 & -\delta_4 & \gamma_4\\-\delta_4 & \beta_4 & -\gamma_4\\\gamma_4 & -\gamma_4 & \alpha_4\end{pmatrix}$	0 – 26 $\frac{a}{2}(2,2,2)$ $\frac{a}{2}(-2,-2,-2)$	$-\begin{pmatrix}\alpha_5 & \beta_5 & \beta_5\\\beta_5 & \alpha_5 & \beta_5\\\beta_5 & \beta_5 & \alpha_5\end{pmatrix}$	0 – 27 $\frac{a}{2}(-2,2,2)$ $\frac{a}{2}(2,-2,-2)$	$-\begin{pmatrix}\alpha_5 & -\beta_5 & -\beta_5\\-\beta_5 & \alpha_5 & \beta_5\\-\beta_5 & \beta_5 & \alpha_5\end{pmatrix}$
0 – 28 $\frac{a}{2}(2,-2,2)$ $\frac{a}{2}(-2,2,-2)$	$-\begin{pmatrix}\alpha_5 & -\beta_5 & \beta_5\\-\beta_5 & \alpha_5 & -\beta_5\\\beta_5 & -\beta_5 & \alpha_5\end{pmatrix}$	0 – 29 $\frac{a}{2}(2,2,-2)$ $\frac{a}{2}(-2,-2,2)$	$-\begin{pmatrix}\alpha_5 & \beta_5 & -\beta_5\\\beta_5 & \alpha_5 & -\beta_5\\-\beta_5 & -\beta_5 & \alpha_5\end{pmatrix}$	0 – 30 $\frac{a}{2}(4,0,0)$ $\frac{a}{2}(-4,0,0)$	$-\begin{pmatrix}\alpha_6 & 0 & 0\\0 & \beta_6 & 0\\0 & 0 & \beta_6\end{pmatrix}$
0 – 31 $\frac{a}{2}(0,4,0)$ $\frac{a}{2}(0,-4,0)$	$-\begin{pmatrix}\beta_6 & 0 & 0\\0 & \alpha_6 & 0\\0 & 0 & \beta_6\end{pmatrix}$	0 – 32 $\frac{a}{2}(0,0,4)$ $\frac{a}{2}(0,0,-4)$	$-\begin{pmatrix}\beta_6 & 0 & 0\\0 & \beta_6 & 0\\0 & 0 & \alpha_6\end{pmatrix}$	0 – 33 $\frac{a}{2}(1,3,3)$ $\frac{a}{2}(-1,-3,-3)$	$-\begin{pmatrix}\alpha_7 & \gamma_7 & \gamma_7\\\gamma_7 & \beta_7 & \delta_7\\\gamma_7 & \delta_7 & \beta_7\end{pmatrix}$
0 – 34 $\frac{a}{2}(-1,3,3)$ $\frac{a}{2}(1,-3,-3)$	$-\begin{pmatrix}\alpha_7 & -\gamma_7 & -\gamma_7\\-\gamma_7 & \beta_7 & \delta_7\\-\gamma_7 & \delta_7 & \beta_7\end{pmatrix}$	0 – 35 $\frac{a}{2}(1,3,-3)$ $\frac{a}{2}(-1,-3,3)$	$-\begin{pmatrix}\alpha_7 & \gamma_7 & -\gamma_7\\\gamma_7 & \beta_7 & -\delta_7\\-\gamma_7 & -\delta_7 & \beta_7\end{pmatrix}$	0 – 36 $\frac{a}{2}(1,-3,3)$ $\frac{a}{2}(-1,3,-3)$	$-\begin{pmatrix}\alpha_7 & -\gamma_7 & \gamma_7\\-\gamma_7 & \beta_7 & -\delta_7\\\gamma_7 & -\delta_7 & \beta_7\end{pmatrix}$
0 – 37 $\frac{a}{2}(3,1,3)$ $\frac{a}{2}(-3,-1,-3)$	$-\begin{pmatrix}\beta_7 & \gamma_7 & \delta_7\\\gamma_7 & \alpha_7 & \gamma_7\\\delta_7 & \gamma_7 & \beta_7\end{pmatrix}$	0 – 38 $\frac{a}{2}(3,-1,-3)$ $\frac{a}{2}(-3,1,3)$	$-\begin{pmatrix}\beta_7 & -\gamma_7 & -\delta_7\\-\gamma_7 & \alpha_7 & \gamma_7\\-\delta_7 & \gamma_7 & \beta_7\end{pmatrix}$	0 – 39 $\frac{a}{2}(3,-1,3)$ $\frac{a}{2}(-3,1,-3)$	$-\begin{pmatrix}\beta_7 & -\gamma_7 & \delta_7\\-\gamma_7 & \alpha_7 & -\gamma_7\\\delta_7 & -\gamma_7 & \beta_7\end{pmatrix}$
0 – 40 $\frac{a}{2}(3,1,-3)$ $\frac{a}{2}(-3,-1,3)$	$-\begin{pmatrix}\beta_7 & \gamma_7 & -\delta_7\\\gamma_7 & \alpha_7 & -\gamma_7\\-\delta_7 & -\gamma_7 & \beta_7\end{pmatrix}$	0 – 41 $\frac{a}{2}(3,3,1)$ $\frac{a}{2}(-3,-3,-1)$	$-\begin{pmatrix}\beta_7 & \delta_7 & \gamma_7\\\delta_7 & \beta_7 & \gamma_7\\\gamma_7 & \gamma_7 & \alpha_7\end{pmatrix}$	0 – 42 $\frac{a}{2}(3,-3,-1)$ $\frac{a}{2}(-3,3,1)$	$-\begin{pmatrix}\beta_7 & -\delta_7 & -\gamma_7\\-\delta_7 & \beta_7 & \gamma_7\\-\gamma_7 & \gamma_7 & \alpha_7\end{pmatrix}$
0 – 43 $\frac{a}{2}(3,3,-1)$ $\frac{a}{2}(-3,-3,1)$	$-\begin{pmatrix}\beta_7 & \delta_7 & -\gamma_7\\\delta_7 & \beta_7 & -\gamma_7\\-\gamma_7 & -\gamma_7 & \alpha_7\end{pmatrix}$	0 – 44 $\frac{a}{2}(3,-3,1)$ $\frac{a}{2}(-3,3,-1)$	$-\begin{pmatrix}\beta_7 & -\delta_7 & \gamma_7\\-\delta_7 & \beta_7 & -\gamma_7\\\gamma_7 & -\gamma_7 & \alpha_7\end{pmatrix}$	0 – 45 $\frac{a}{2}(4,2,0)$ $\frac{a}{2}(-4,-2,0)$	$-\begin{pmatrix}\alpha_8 & \delta_8 & 0\\\delta_8 & \beta_8 & 0\\0 & 0 & \gamma_8\end{pmatrix}$

0 – 46 $\frac{a}{2}(4,-2,0)$ $\frac{a}{2}(-4,2,0)$	$-\begin{pmatrix} \alpha_8 & -\delta_8 & 0 \\ -\delta_8 & \beta_8 & 0 \\ 0 & 0 & \gamma_8 \end{pmatrix}$	0 – 47 $\frac{a}{2}(4,0,2)$ $\frac{a}{2}(-4,0,-2)$	$-\begin{pmatrix} \alpha_8 & 0 & \delta_8 \\ 0 & \gamma_8 & 0 \\ \delta_8 & 0 & \beta_8 \end{pmatrix}$	0 – 48 $\frac{a}{2}(4,0,-2)$ $\frac{a}{2}(-4,0,2)$	$-\begin{pmatrix} \alpha_8 & 0 & -\delta_8 \\ 0 & \gamma_8 & 0 \\ -\delta_8 & 0 & \beta_8 \end{pmatrix}$
0 – 49 $\frac{a}{2}(0,2,4)$ $\frac{a}{2}(0,-2,-4)$	$-\begin{pmatrix} \gamma_8 & 0 & 0 \\ 0 & \beta_8 & \delta_8 \\ 0 & \delta_8 & \alpha_8 \end{pmatrix}$	0 – 50 $\frac{a}{2}(0,2,-4)$ $\frac{a}{2}(0,-2,4)$	$-\begin{pmatrix} \gamma_8 & 0 & 0 \\ 0 & \beta_8 & -\delta_8 \\ 0 & -\delta_8 & \alpha_8 \end{pmatrix}$	0 – 51 $\frac{a}{2}(0,4,2)$ $\frac{a}{2}(0,-4,-2)$	$-\begin{pmatrix} \gamma_8 & 0 & 0 \\ 0 & \alpha_8 & \delta_8 \\ 0 & \delta_8 & \beta_8 \end{pmatrix}$
0 – 52 $\frac{a}{2}(0,-4,2)$ $\frac{a}{2}(0,4,-2)$	$-\begin{pmatrix} \gamma_8 & 0 & 0 \\ 0 & \alpha_8 & -\delta_8 \\ 0 & -\delta_8 & \beta_8 \end{pmatrix}$	0 – 53 $\frac{a}{2}(2,4,0)$ $\frac{a}{2}(-2,-4,0)$	$-\begin{pmatrix} \beta_8 & \delta_8 & 0 \\ \delta_8 & \alpha_8 & 0 \\ 0 & 0 & \gamma_8 \end{pmatrix}$	0 – 54 $\frac{a}{2}(2,-4,0)$ $\frac{a}{2}(-2,4,0)$	$-\begin{pmatrix} \beta_8 & -\delta_8 & 0 \\ -\delta_8 & \alpha_8 & 0 \\ 0 & 0 & \gamma_8 \end{pmatrix}$
0 – 55 $\frac{a}{2}(2,0,4)$ $\frac{a}{2}(-2,0,-4)$	$-\begin{pmatrix} \beta_8 & 0 & \delta_8 \\ 0 & \gamma_8 & 0 \\ \delta_8 & 0 & \alpha_8 \end{pmatrix}$	0 – 56 $\frac{a}{2}(2,0,-4)$ $\frac{a}{2}(-2,0,4)$	$-\begin{pmatrix} \beta_8 & 0 & -\delta_8 \\ 0 & \gamma_8 & 0 \\ -\delta_8 & 0 & \alpha_8 \end{pmatrix}$	0 – 57 $\frac{a}{2}(4,2,2)$ $\frac{a}{2}(-4,-2,-2)$	$-\begin{pmatrix} \alpha_9 & \gamma_9 & \gamma_9 \\ \gamma_9 & \beta_9 & \delta_9 \\ \gamma_9 & \delta_9 & \beta_9 \end{pmatrix}$
0 – 58 $\frac{a}{2}(-4,2,2)$ $\frac{a}{2}(4,-2,-2)$	$-\begin{pmatrix} \alpha_9 & -\gamma_9 & -\gamma_9 \\ -\gamma_9 & \beta_9 & \delta_9 \\ -\gamma_9 & \delta_9 & \beta_9 \end{pmatrix}$	0 – 60 $\frac{a}{2}(2,4,-2)$ $\frac{a}{2}(-2,-4,2)$	$-\begin{pmatrix} \beta_9 & \gamma_9 & -\delta_9 \\ \gamma_9 & \alpha_9 & -\gamma_9 \\ -\delta_9 & -\gamma_9 & \beta_9 \end{pmatrix}$	0 – 61 $\frac{a}{2}(2,4,2)$ $\frac{a}{2}(-2,-4,-2)$	$-\begin{pmatrix} \beta_9 & \gamma_9 & \delta_9 \\ \gamma_9 & \alpha_9 & \gamma_9 \\ \delta_9 & \gamma_9 & \beta_9 \end{pmatrix}$
0 – 62 $\frac{a}{2}(2,-4,2)$ $\frac{a}{2}(-2,4,-2)$	$-\begin{pmatrix} \beta_9 & -\gamma_9 & -\delta_9 \\ -\gamma_9 & \alpha_9 & \gamma_9 \\ -\delta_9 & \gamma_9 & \beta_9 \end{pmatrix}$	0 – 63 $\frac{a}{2}(2,4,-2)$ $\frac{a}{2}(-2,-4,2)$	$-\begin{pmatrix} \beta_9 & \gamma_9 & -\delta_9 \\ \gamma_9 & \alpha_9 & -\gamma_9 \\ -\delta_9 & -\gamma_9 & \beta_9 \end{pmatrix}$	0 – 64 $\frac{a}{2}(2,-4,2)$ $\frac{a}{2}(-2,4,-2)$	$-\begin{pmatrix} \beta_9 & -\gamma_9 & \delta_9 \\ -\gamma_9 & \alpha_9 & -\gamma_9 \\ \delta_9 & -\gamma_9 & \beta_9 \end{pmatrix}$
0 – 65 $\frac{a}{2}(2,2,4)$ $\frac{a}{2}(-2,-2,-4)$	$-\begin{pmatrix} \beta_9 & \delta_9 & \gamma_9 \\ \delta_9 & \beta_9 & \gamma_9 \\ \gamma_9 & \gamma_9 & \alpha_9 \end{pmatrix}$	0 – 66 $\frac{a}{2}(-2,2,4)$ $\frac{a}{2}(2,-2,-4)$	$-\begin{pmatrix} \beta_9 & -\delta_9 & -\gamma_9 \\ -\delta_9 & \beta_9 & \gamma_9 \\ -\gamma_9 & \gamma_9 & \alpha_9 \end{pmatrix}$	0 – 67 $\frac{a}{2}(2,2,-4)$ $\frac{a}{2}(-2,-2,4)$	$-\begin{pmatrix} \beta_9 & \delta_9 & -\gamma_9 \\ \delta_9 & \beta_9 & -\gamma_9 \\ -\gamma_9 & -\gamma_9 & \alpha_9 \end{pmatrix}$
0 – 68 $\frac{a}{2}(2,-2,4)$ $\frac{a}{2}(-2,2,-4)$	$-\begin{pmatrix} \beta_9 & -\delta_9 & \gamma_9 \\ -\delta_9 & \beta_9 & -\gamma_9 \\ \gamma_9 & -\gamma_9 & \alpha_9 \end{pmatrix}$	0 – 69 $\frac{a}{2}(3,3,3)$ $\frac{a}{2}(-3,-3,-3)$	$-\begin{pmatrix} \alpha_{10} & \beta_{10} & \beta_{10} \\ \beta_{10} & \alpha_{10} & \beta_{10} \\ \beta_{10} & \beta_{10} & \alpha_{10} \end{pmatrix}$	0 – 70 $\frac{a}{2}(-3,3,3)$ $\frac{a}{2}(3,-3,-3)$	$-\begin{pmatrix} \alpha_{10} & -\beta_{10} & -\beta_{10} \\ -\beta_{10} & \alpha_{10} & \beta_{10} \\ -\beta_{10} & \beta_{10} & \alpha_{10} \end{pmatrix}$
0 – 71 $\frac{a}{2}(3,-3,3)$ $\frac{a}{2}(-3,3,-3)$	$-\begin{pmatrix} \alpha_{10} & -\beta_{10} & \beta_{10} \\ -\beta_{10} & \alpha_{10} & -\beta_{10} \\ \beta_{10} & -\beta_{10} & \alpha_{10} \end{pmatrix}$	0 – 72 $\frac{a}{2}(3,3,-3)$ $\frac{a}{2}(-3,-3,3)$	$-\begin{pmatrix} \alpha_{10} & \beta_{10} & -\beta_{10} \\ \beta_{10} & \alpha_{10} & -\beta_{10} \\ -\beta_{10} & -\beta_{10} & \alpha_{10} \end{pmatrix}$		

4.0 CONCLUSION

The dispersion curves and thermodynamic properties of Cr and Nb were calculated successfully using two techniques; the interatomic force constants (IFCs) technique employing the Born – von Kármán model and the first principle technique based on DFT implemented by QUANTUM ESPRESSO. The phonon dispersions were computed along the principal symmetry directions of the BZ. The results obtained from both techniques were matched with data from experiment. We conclude that the phonon dispersion curve of Cr and Nb from IFCs calculation shows a close agreement with experiment just like that from the first principle calculations. In the first principle calculations for Cr using DFT, the GGA (PAW) functional gave a better result compared to GGA (PBE) with the PW91 worst of the functionals and for Nb the PW91 functional shows a close result to experiment, when compared to computational. GGA (PBE) giving better results to LDA functional.

REFERENCES

[1] Da Cunha Lima, I. C., Brescansin, L. M and Shukla, M. M. (1974). Lattice Dynamics of Alkali Metals. *Physica* 72, 179 – 187.

[2] Baroni, S., de Gironcoli, S., Dal Corso, A. and Giannozzi. P. (2001). Phonons and related crystal properties from density-functional perturbation theory. *Rev. Mod. Phys*., 73:515

[3] Born, M. and Huang, K. (1954). *Dynamical Theory of Crystal Lattices*, Oxford, Clarendon Press, p 420

[4] De Cicco, P. D. and Johnson, F. A. (1969). The quantum theory of lattice dynamics. IV. *Proc. R. Soc. London, Ser.* A 310, 111

[5] Pick, R., Cohen, M. H. and Martin, R. M. (1970). Microscopic theory of force constants in the adiabatic approximation. *Phys. Rev*. B 1, 910.

[6] Michel, K. H., Çakır,D., Sevik,C. and Peeters, F. M. (2017). Piezoelectricity in two-dimensional materials: a comparative study between lattice dynamics and ab-initio calculations. *Cond-Mat. Mtrl-Sci*. 1703.

[7] Phillips, J. C. and Kleinman, L. (1959). New method for calculating wave functions in crystals and molecules. *Phys. Rev*. 116, 287

[8] Antonick, E. (1959). Approximate formulation of the orthogonalized plane-wave method. *J. Phys. Chem. Solids* 10, 314

[9] Vosko, S. H., Taylor, R., and Keech, G. H. (1965). Effective Charge Associated with a Displaced Ion in the Orthogonalized-Plane-Wave Formalism. *Can. J. Phys.* 43, 1187

[10] Animalu, A. O. E. (1966). The total electronic band structure energy for 29 elements. *Proc. Roy. Soc.* A294, 376

[11] Animalu, A. O. E. and Heine, V. (1965). The screened model potential for 25 elements. *Philos. Mag*. 12, 1249

[12] Abarenkov, I. V. and Heine, V. (1965). The model potential for positive ions. *Phil. Mag.* 12, 529-537

[13] Harrison, W. A. (1969). Transition-metal pseudopotentials. *Phys. Rev.* 181, 1036

[14] Heine, V. and Abarenkov, I. V. (1964). A new method for the electronic structure of metals. *Philos. Mag,* 9, 465

[15] Animalu, A. O. E. (1974). Electronic structure of transition metals. III. *d*-band resonance and Regge-pole theory. *Phys. Rev*. B 10, 4964.

[16] Animalu, A. O. E. (1973). Electronic structure of transition metals. II. Phonon spectra. *Phys. Rev*. B 8, 3555

[17] Baroni, S., de Gironcoli, S., Dal Corso, A. and Giannozzi. P. (2001). Phonons and related crystal properties from density-functional perturbation theory. *Rev. Mod. Phys*., 73:515

[18] Dal Corso, A. and de Gironcoli, S. (2000). *Ab initio* phonon dispersions of Fe and Ni. *Phys. Rev.* B 62, 273

[19] Heid, R., and Bohnen, K. P. (1999). Linear response in a density-functional mixed-basis approach. *Phys. Rev*. B 60, R3709

[20] Dal Corso, A., Pasquarello, A. and Baldereschi, A. (1997). Density-functional perturbation theory for lattice dynamics with ultra-soft pseudopotentials. *Phys. Rev*. B 56, R11369

[21]   Savrasov, S. Y. and Savrasov, D. Y. (1996). Electron-phonon interactions and related physical properties of metals from linear-response theory. *Phys. Rev*. B 54, 16487

[22]   de Gironcoli, S. (1995). Lattice dynamics of metals from density-functional perturbation theory. *Phys. Rev*. B 51, 6773

[23]   Grabowski, B., Hickel, T. and Neugebauer, J. (2007). *Ab initio* study of the thermodynamic properties of nonmagnetic elementary fcc metals: Exchange-correlation-related error bars and chemical trends. *Phys. Rev*. B 76, 024309

[24]   Favot, F. and Dal Corso, A. (1999). Phonon dispersions: Performance of the generalized gradient approximation. *Phys. Rev*. B 60, 11427

[25]   Dal Corso, A. (2013). Ab initio phonon dispersions of transition and noble metal: effects of the exchange and correlation functional. *J. Phys.: Condensed Matter*, 25, 1-9

[26]   Margine, E. R., Lambert, H. and Giustino, F. (2016). Electron-Phonon Interaction and Pairing Mechanism in the Superconducting Ca-Intercalated Bilayer Graphene. *Scientific Reports*, 6, 21414

[27]   Al Taleb, A. and Farias, D. (2016). Phonon Dynamics of Graphene on Metals. *Journal of Physics: Condensed Matter*, 28, 10

[28]   Alessandro, E., Jefferson, M. and Bartolomeo C. (2016). Thermal properties of molecular crystals through dispersion-corrected quasi-harmonic ab initio calculations: the case of urea. *Chem. Commun.* 52, 1820

[29]   Press, W. H., Teukolsky, S. A., Vetterling, W. T. and Flannery, B. P. (1989). *Numerical Recipes: The Art of Scientific Computing* (Cambridge University Press, Cambridge, U.K.).

[30]   Gilat, G. and Raubenheimer, L. T. (1966). Accurate numerical method for calculating frequency-distribution functions in solids. *Phys. Rev*. 144, 390

[31]   Giannozzi, P., Baroni, S., Bonini, N., Calandra, M., Car, R., Cavazzoni, C., Ceresoli, D., Chiarotti, G. L., Cococcioni, M., Dabo, I., Dal Corso, A., Fabris, S., Fratesi, G., de Gironcoli, S., Gebauer, R., Gerstmann, U., Gougoussis, C., Kokalj, A., Lazzeri, M., Martin-Samos, L., Marzari, N., Mauri, F., Mazzarello, R., Paolini, S., Pasquarello, A., Paulatto, L., Sbraccia, C., Scandolo, S., Sclauzero, G., Seitsonen, A. P., Smogunov, A., Umari, P. and Wentzcovitch, R. M. (2009). QUANTUM ESPRESSO: a modular and open-source software project for quantum simulations of materials. *J. Phys.: Condens. Matter* **21**, 395502.

[32]   Giannozzi, P., Andreussi, O., Brumme, T, Bunau, O., Nardelli, M. B., Calandra, M., Car, R., Cavazzoni, C., Ceresoli, D., Cococcioni, M., Colonna, N., Carnimeo, I., Dal Corso, A., de Gironcoli, S., Delugas, P., DiStasio Jr, R. A., Ferretti, A., Floris, A., Fratesi, G., Fugallo, G., Gebauer, R., Gerstmann, U., Giustino, F., Gorni, T., Jia, J., Kawamura, M., Ko, H-Y., Kokalj, A ., Küçükbenli, E., Lazzeri, M., Marsili, M., Marzari, N., Mauri, F., Nguyen, N. L., Nguyen, H-V., Otero-de-la-Roza, A., Paulatto, L., Poncé, S., Rocca, D., Sabatini, R., Santra, B., Schlipf, M ., Seitsonen, A. P., Smogunov, A., Timrov, I., Thonhauser, T., Umari, P., Vast, N., Wu, X., and Baroni, S. (2017). Advanced capabilities for materials modelling with Quantum ESPRESSO. *J. Phys.: Condensed. Matter.* Vol. 29. **24.**

[33]   Landau, L. D. and Lifshitz, E. M. (1980). *Statistical Physics*, 3rd. ed. (Pergamon, London), Pt. 1, Pp. 193

[34]   Changyol, L. and Xavier, G. (1995). Ab initio calculation of the thermodynamic properties and atomic temperature factors of SiO_2 α-quartz and stishovite. *Phys. Rev*. B 51, 8610

[35]   Bolef, D. I. and De Klerk, J. (1963). Anomalies in the elastic constants and thermal   expansion of chromium single crystals. *Phys. Rev*., 129, 1063

[36]   Nakagawa Y. and Woods A. D. B., (1963). Lattice dynamics of niobium. *Phys. Rev. Letters* 11, 6, 271-274.